

---

# Encoding Involutory Invariance in Neural Networks

---

**Anwesh Bhattacharya\***

Department of Physics, Department of CS&IS  
Birla Institute of Technology & Science Pilani  
Pilani, Rajasthan, India - 333031  
f2016590@pilani.bits-pilani.ac.in

**Marios Mattheakis, Pavlos Protopapas**

John A. Paulson School of Engineering and Applied Sciences, Harvard University  
Cambridge, Massachusetts 02138, United States  
mariosmat@seas.harvard.edu, pavlos@seas.harvard.edu

## Abstract

In certain situations, Neural Networks (NN) are trained upon data that obey underlying physical symmetries. However, it is not guaranteed that NNs will obey the underlying symmetry unless embedded in the network structure. In this work, we explore a special kind of symmetry where functions are invariant with respect to involutory linear/affine transformations up to parity  $p = \pm 1$ . We develop mathematical theorems and propose NN architectures that ensure invariance and universal approximation properties. Numerical experiments indicate that the proposed models outperform baseline networks while respecting the imposed symmetry. An adaption of our technique to convolutional NN classification tasks for datasets with inherent horizontal/vertical reflection symmetry has also been proposed.

## 1 Introduction

There has been notable effort in the direction of encoding physical symmetries in NNs. [1] encodes symmetries in NNs that make it capable of learning even/odd functions, and other techniques (*Symplectic Neural Networks*) that guarantee energy conservation. [2] explore techniques to solve the Navier-Stokes equations while guaranteeing its various symmetries — space/time translation, rotation, reflection and scaling. [3] build networks that obey equivariance to Lorenz Transformations [4] which is essential in problems centred around Particle Physics. [5] experiment with feeding NNs art paintings and conduct a Principal Component Analysis (PCA) on the weights of the final dense layer of the network. They have found that the distribution of the weights reflect the underlying symmetries of the images. [6] proposes novel architectures for graph networks that are equivariant to the Euclidean group.

Significant effort has been spent on guaranteeing continuous group symmetries such as [7] which compute rotation invariant feature maps for 3-D CAD models. [8] have developed neural networks with generalized group-theoretic features such as G-convolutions. A theoretical analysis of the connection between group convolutions and equivariance with respect to actions of a group can be found in [9]. Although these works are significant and sophisticated on their own right in making NNs equivariant with respect to group actions, we present a simpler alternative with a standard Feed-Forward Neural Network (FFNN) [10] that guarantees involutory invariance. Is there a set of

---

\*Use footnote for providing further information about author (webpage, alternative address)—*not* for acknowledging funding agencies.

transformations, that are physically useful and relevant, such that encoding invariance to them is *simple*?

### 1.1 Why Involutory Transformations?

An involutory transformation is one such that its inverse is itself. They have properties that make it conducive for standard FFNNs, after minimalist changes, to obey invariance with respect to them. Universal Approximation properties [11] for single hidden layer neural networks holds as a natural consequence, and for deeper networks also follow should the conditions in [12] also be obeyed.

Reflection about a line  $y = mx$  in 2-D and inversion about the origin in N-D space are physically important transformations, which belong to the class of involutory *linear* transformations (represented by  $A$  hereon in this work) The techniques developed are also applicable to involutory *affine* transformations, after suitable modification. This allows NNs to learn reflection about lines not passing through the origin ( $y = mx + c$ ) or inversion about an arbitrary points.<sup>2</sup>

### 1.2 Organization of the Paper

We first present some preliminaries of linear algebra in Section A. Subsequently, in Section B we prove the *Involutory Partition Theorem* that endows FFNNs the capability of respecting involutory invariances and universal approximation properties in the space of function with such invariances. Then we present various symmetry-encoded architectures in Section 2 including a mathematical analysis of *Involutory Summarized* activation functions — a simple technique of superposing arbitrary activation functions in manner that guarantees invariance. Section 3 contains experimental results on various test problems. Future directions of research are discussed in Section 5 and we conclude in Section 6

## 2 The Proposed Architectures

### 2.1 Extending the Hub Network (HN) to Involutory Symmetries

Mattheakis et. al. [1] define a hub-layered neural network that respects an even/odd symmetry about a fixed point and learns a function  $f : \mathbb{R} \rightarrow \mathbb{R}$ . Let the activation value of  $i^{\text{th}}$  node in the final hidden layer of the neural network be denoted as  $h_i(x)$  for an input  $x$ . The output  $V(x)$  of a vanilla neural network would be —

$$V(x) = \sum_i w_i h_i(x) + b$$

If one superimposes the final hidden layers' activations as  $H^\pm(x) = h_i(x) \pm h_i(-x)$ , then a hub-layered neural network  $H(x)$  could be constructed as follows —

$$H_{\text{even}}(x) = \sum_i w_i H^+(x) + 2b$$

It can be confirmed that  $H_{\text{even}}(x) = H_{\text{even}}(-x)$ . An odd function could be learnt by —

$$H_{\text{odd}}(x) = \sum_i w_i H^-(x)$$

There is no need for a bias to be learnt if the underlying data is odd. It can also be confirmed that  $H_{\text{odd}}(x) = -H_{\text{odd}}(-x)$ . The architecture is easily extended so that it can learn functions  $\mathbb{R}^n \rightarrow \mathbb{R}$ , that are invariant to an involutory transformation,  $A$ , up to parity  $p = \pm 1$  by constructing the hub layer as follows —

$$H^p(X) = h_i(X) + p h_i(AX)$$

Accordingly, the network output is —

$$NN_{A;p}(X) = \sum_i w_i H^p(X) + \theta(p) \times 2b$$

where  $\theta$  is the heaviside step function. It can be confirmed that  $NN_{A;p}(AX) = p NN_{A;p}(X)$ .

<sup>2</sup>Refer to section 2.3.3 for a discussion on this subtle aspect.

## 2.2 Reducing Double Computations by Summarized Activation Network (SAN)

The hub-layered neural network requires two forward passes up to the last hidden layer (for  $X$  and  $AX$ ) before their activations are summed by the final hidden layer. The guarantee of symmetry comes at a computational cost. It would be desirable to eliminate the double computations entirely.

The double computation cost for the baseline hub architecture grows as the depth of the network. Thus, limiting the double computations up to a pre-specified depth would remove the dependence of the cost on the depth. In order to achieve this, the crucial observation is: *it is sufficient to guarantee that the activations in any specified hidden layer is invariant to the involutory transformation to guarantee the invariance of the network output.*

Let  $p = \pm 1$  be the parity to be respected. In the case of 1-D invariances, this requires  $a_i^{[l]}(-x) = pa_i^{[l]}(x)$  for the  $i^{\text{th}}$  node of the  $l^{\text{th}}$  layer. To minimize double computations, the invariance can be encoded at  $l = 1$ .

This is achieved by setting —

$$a_i^{[1]}(x) = \sigma(w_i x + b) + p\sigma(-w_i x + b)$$

which guarantees  $a_i^{[1]}(-x) = pa_i^{[1]}(x)$ . Extending this to generic  $N$ -dimensional involutions, one can use —

$$a_i^{[1]}(X) = \sigma(w^T X + b) + p\sigma(w^T AX + b)$$

It is easily seen that  $a_i^{[1]}(AX) = pa_i^{[1]}(X)$ . Such a superposition of activation functions as the one given above is called an *involutory symmetrized* activation.

### 2.2.1 The Class of Safe Activation Functions

We noticed a peculiarity in the development of our architectures while learning even functions in 1-D. Denote  $a_i^{[1]}$  as the activation of the  $i^{\text{th}}$  node in the first hidden layer,  $i \in \{1, 2, \dots, l_{\text{hidden}}\}$ . We fixed the bias parameter to zero in our initial experimentation and used `sigmoid` activation. However, it was noted that the final function that the network learned,  $NN(x)$  lacked any variation in  $x$  — *there was a lack in expressivity*. Let pre-activation value be  $a_i^{[1]}(x) = \sigma(w_i x) + \sigma(-w_i x)$  and let  $z_i$  be a variable,  $z_i = w_i x$  for some weight  $w_i$ . Since  $a_i^{[1]}(x)$  is even, the network output is also even. It is a property of `sigmoid` that —

$$\begin{aligned} \sigma(z) + \sigma(-z) &= \frac{1}{1 + e^{-z}} + \frac{1}{1 + e^z} = 1 \\ \implies \frac{\partial a_i^{[1]}}{\partial x} &= \frac{da_i^{[1]}}{dz_i} \frac{\partial z_i}{\partial x} = \left\{ \frac{d}{dz} [\sigma(z) + \sigma(-z)] \right\} \Big|_{z=z_i} \frac{\partial z_i}{\partial x} = 0 \\ \implies \frac{\partial a_i^{[1]}}{\partial w_i} &= \frac{da_i^{[1]}}{dz_i} \frac{\partial z_i}{\partial w_i} = \left\{ \frac{d}{dz} [\sigma(z) + \sigma(-z)] \right\} \Big|_{z=z_i} \frac{\partial z_i}{\partial w_i} = 0 \end{aligned}$$

Hence, the first layer weights are frozen in training. Since  $i$  was chosen arbitrarily, the NN learns a constant function because *all* the activations in the first hidden-layer are independent of the input  $x$ . This is precisely the lack of expressivity that was attributed to —

$$\forall i \in \{1, 2, \dots, l_{\text{hidden}}\} \ni \frac{\partial a_i^{[1]}}{\partial x} = 0 \implies NN(x) \text{ is a constant function in } \mathbb{R}$$

One can generalize this to the  $n$  dimensional case. Let  $f : \mathbb{R}^n \rightarrow \mathbb{R}$  and the involutory invariance to be respected be  $A \in \mathbb{R}^{n \times n}$ , and the activation function in the first layer be denoted by  $\sigma$ . For  $X, w_i \in \mathbb{R}$ , and  $b \in \mathbb{R}$  (*without restricting the bias to any particular value*), the activation value of the  $i^{\text{th}}$  node in the first hidden layer —

$$\begin{aligned} a_i^{[1]} &= \sigma(b + w_i^T X) + \sigma(b + w_i^T AX) \\ \nabla_X a_i^{[1]} &= [\sigma'(b + w_i^T X)I_n + \sigma'(b + w_i^T AX)A^T] w_i \end{aligned}$$

where we define  $\sigma'$  as the derivative of  $\sigma$ . Let  $z = w_i^T X$  be a uni-dimensional variable. It covers the full range of  $\mathbb{R}$  as we premise that  $X, w_i$  are arbitrary. For the NN to retain expressivity,  $\nabla_X a_i^{[1]} \neq \vec{0}_n$ . On assuming the contrary, it can be seen that it is possible if the matrix in [ ] is the zero matrix. This prevents  $A$  from having any off-diagonal elements, only allowing  $A = -I_n$  —

$$\begin{aligned}\sigma'(b + w_i^T X) - \sigma'(b - w_i^T X) &= 0 \\ \int \sigma'(b + z) dz - \int \sigma'(b - z) dz &= 0 \\ \sigma(b + z) + \sigma(b - z) &= C \\ \left[ \sigma(b^* + z) - \frac{C}{2} \right] &= - \left[ \sigma(b^* - z) - \frac{C}{2} \right]\end{aligned}$$

where  $C \in \mathbb{R}$  is a constant of integration. Moreover, such a situation could only occur if there existed a point  $b^*$ , about which the condition  $\sigma(b^* + z) + \sigma(b^* - z) = C \forall z \in \mathbb{R}$ . Substituting  $z = 0$  (since  $z$  is a free variable), we get  $C = 2\sigma(b^*)$ . If we define a new function  $\sigma_{b^*}(z) = \sigma(b^* + z) - \sigma(b^*)$ , we obtain —

$$\sigma_{b^*}(z) = -\sigma_{b^*}(-z)$$

In other words, the activation  $\sigma$  is odd about  $b^*$  — after an appropriate shift by  $\sigma(b^*)$ . During training, if the bias assumes a value of  $b^*$ , the training freezes because —

$$\begin{aligned}\nabla_{w_i} a_i^{[1]} &= [\sigma'(b + w_i^T X)I_n + \sigma'(b + w_i^T AX)A^T] X \\ &= \vec{0}_n\end{aligned}$$

for all nodes  $i$  in the first hidden layer. This chokes the expressivity of the NN significantly by restricting it to learn constant functions in  $\mathbb{R}^n$ . In the particular case of the sigmoid function,  $b^* = 0$ . It belongs to a wider class of functions, all of which *could* restrict the expressivity of neural networks while learning an inversion invariance ( $-I_n$ ). Define —

$$\begin{aligned}\text{INV-UNSAFE} &= \{ \sigma \mid \sigma : \mathbb{R} \rightarrow \mathbb{R}; \exists b^* \ni \sigma_{b^*}(z) \text{ is odd where } \sigma_{b^*}(z) = \sigma(b^* + z) - \sigma(b^*) \} \\ \text{INV-SAFE} &= \{ \sigma \mid \sigma : \mathbb{R} \rightarrow \mathbb{R}; \nexists b^* \ni \sigma_{b^*}(z) \text{ is odd where } \sigma_{b^*}(z) = \sigma(b^* + z) - \sigma(b^*) \}\end{aligned}$$

Note that these two classes of functions are complements of each other. In [13], a variant of the snake activation function is used where  $\sigma(z) = z + \sin z$  and this contains infinitely many *unsafe* points,  $b^* = \pm n\pi$  for  $n \in \mathbb{W}$  —

$$\begin{aligned}\sigma_{b^*}(z) &= \sigma(\pm n\pi + z) - \sigma(\pm n\pi) \\ &= (\pm n\pi + z) + \sin(\pm n\pi + z) \mp n\pi - \sin(\pm n\pi) \\ &= (-1)^n \sin(z)\end{aligned}$$

which is clearly an odd function. Hence **snake**  $\in$  INV-UNSAFE. Similarly, **tanh**  $\in$  INV-UNSAFE.

**Result** : ReLU[14], swish[15], softplus[16]  $\in$  INV-SAFE.

**Proof** : Assume  $\exists b^*$  such that  $\sigma_{b^*}(z) = \sigma(b^* + z) - \sigma(b^*)$  is odd. The concerned activation functions have the following behaviour —

$$\begin{aligned}\lim_{z \rightarrow \infty} \sigma_{b^*}(z) &= \infty \\ \lim_{z \rightarrow -\infty} \sigma_{b^*}(z) &= 0\end{aligned}$$

Due to their asymptotic/diverging behaviour as  $z \rightarrow \pm\infty$ , it is possible to state —

$$\begin{aligned}\exists L > 1, \exists z_+ > 0 \ni z \geq z_+ &\implies \sigma_{b^*}(z) \geq L \\ \exists 0 \leq \epsilon < 1, \exists z_- < 0 \ni z \leq z_- &\implies |\sigma_{b^*}(z)| \leq \epsilon\end{aligned}$$

We are free to choose an  $L$  sufficiently large, and an  $\epsilon$  sufficiently small. Define a new variable  $z^* = \max(|z_+|, |z_-|) \implies z^* \geq z_+$  and  $-z^* \leq z_-$ . This would imply —

$$\begin{aligned}1 < L \leq \sigma_{b^*}(z^*) \text{ and } |\sigma_{b^*}(-z^*)| &\leq \epsilon < 1 \\ \implies \sigma_{b^*}(-z^*) &\neq -\sigma_{b^*}(z^*)\end{aligned}$$

Hence, for any  $b^*$  it is always possible to find a point  $z^*$  about which the function fails to be odd. Hence `ReLU`, `swish`, `softplus`  $\in$  `INV-SAFE`. To show that other activations are *safe*, one would need to follow a proof along similar lines.

We have considered functions obeying inversion invariance with an even parity. A similar derivation can be carried out for the case of odd parity —

$$\begin{aligned}\sigma'(b + w_i^T X) + \sigma'(b - w_i^T X) &= 0 \\ \int \sigma'(b + z) dz + \int \sigma'(b - z) dz &= 0 \\ \sigma(b + z) - \sigma(b - z) &= C\end{aligned}$$

By setting  $z = 0$ , we obtain  $C = 0$  and the condition reduces to (*for an appropriate  $b^*$* ) —

$$\sigma(b^* + z) = \sigma(b^* - z)$$

The class of functions would now be (*for odd parity*) —

$$\begin{aligned}\text{INV-UNSAFE}' &= \{\sigma \mid \sigma : \mathbb{R} \rightarrow \mathbb{R}; \exists b^* \ni \sigma_{b^*}(z) \text{ is even where } \sigma_{b^*}(z) = \sigma(b^* + z)\} \\ \text{INV-SAFE}' &= \{\sigma \mid \sigma : \mathbb{R} \rightarrow \mathbb{R}; \nexists b^* \ni \sigma_{b^*}(z) \text{ is even where } \sigma_{b^*}(z) = \sigma(b^* + z)\}\end{aligned}$$

Non-decreasing functions cannot have a point about which they are even, and thus `sigmoid`, `tanh`, `softplus`, `ReLU`  $\in$  `INV-SAFE'`. Although, `swish` is not strictly non-decreasing, it can be shown to belong to `INV-SAFE'` by a similar proof as given previously.<sup>3</sup>

### 2.3 The Involutory Partition Theorem Network (IPTNet)

It would be convenient to avoid any double-pass computations in the neural network while guaranteeing involutory invariance. The motivation of proving the involutory partition theorem can be found by considering the instance of learning a function  $f : \mathbb{R} \rightarrow \mathbb{R}$ . If a function is even/odd, its behaviour on  $\mathbb{R}$  is completely specified by its behaviour on  $\mathbb{R}_+$ . If there happens to be a training example  $(x^{(i)}, y^{(i)})$  where  $x^{(i)} \in \mathbb{R}_-$ , it can be fed to the neural network as  $(-x^{(i)}, p \times y^{(i)})$  instead where  $p = \pm 1$  is the parity. During inference time, if we require the NN output on a point  $z \in \mathbb{R}$ , we reparameterize it as follows —

$$NN(z; p) \leftarrow \begin{cases} NN(z) & z \geq 0 \\ p \times NN(-z) & z < 0 \end{cases}$$

In 1-D, the real number line naturally partitions into  $\mathbb{R}_-, \mathbb{R}_0 = \{0\}, \mathbb{R}_+$ . An even/odd function's behaviour on  $\mathbb{R}$  is solely determined by its behaviour on  $\mathbb{R}_0 \cup \mathbb{R}_+$ . Hence, it would be convenient for a generic involutory transformation  $A$  to also partition  $\mathbb{R}^n$  in an analogous fashion into subsets, say  $(S_-, S_0, S_+)$  —

If such is the case, then one need only feed training examples to the neural network that belong to  $S_0 \cup S_+$  and the invariance properties of the function would be guaranteed. The *Involutory Partition Theorem* shows that such a construction is possible. The theorem is formally stated as —

**Theorem** : An involutory matrix  $A \neq I_n$  partitions  $\mathbb{R}^n$  into three mutually exclusive non-empty subsets  $S_0, S_+, S_-$ , with the following properties —

1.  $\forall \vec{v} \in S_0, A\vec{v} = \vec{v}$
2.  $\forall \vec{v} \in S_+, A\vec{v} \in S_-$
3.  $\forall \vec{v} \in S_-, A\vec{v} \in S_+$

**Proof** : Please refer to appendix B for the proof.

We can feed the neural network training examples as  $(x^{(i)}, y^{(i)})$  if  $x^{(i)} \notin S_-$ . On the other hand, if  $x^{(i)} \in S_-$ , we feed it as  $(Ax^{(i)}, p \times y^{(i)})$ . Similarly, when we require inference on a  $Z \in \mathbb{R}^n$ , the

<sup>3</sup>It is not necessarily true that using an activation function  $\sigma \in \text{INV-UNSAFE}$  or  $\sigma \in \text{INV-UNSAFE}'$  would lead to a lack of expressivity while learning an inversion invariance. In practice, we have found that `sigmoid` is capable of learning functions that obey an inversion invariance with even parity. This is distinctly different from `snake`, however, as it has infinitely many *unsafe* points, and hence an *unwise* choice for an activation function.

reparameterization is —

$$NN(Z; p) \leftarrow \begin{cases} NN(Z) & Z \in S_0 \cup S_+ \\ p \times NN(AZ) & Z \in S_- \end{cases}$$

Essentially, the action of  $f$  in  $\mathbb{R}^n$  is completely specified by considering its action in  $S_0 \cup S_+$ . This is the *Principal Involutory Domain* corresponding to the matrix  $A$ , denoted by  $PID(A)$ .

### 2.3.1 Set Membership Test

Given a training/test vector  $\vec{x}$ , it must be determined whether it belongs to the principal involutory domain of  $A$ . We present an algorithm that determines this in  $\Theta(n\gamma)$  time for one vector.  $\gamma$  is the dimensionality of the  $S_-$  eigensubspace. Since  $n \geq \gamma = \mathcal{O}(n)$ , this makes it  $\mathcal{O}(n^2)$ .

IN-PID( $\vec{v}$ ,  $Pinv$ ,  $\gamma$ )

```

1   $n \leftarrow Pinv.dimensions$ 
2  for  $\vec{r}$  in  $Pinv.rows[n, \dots, n - \gamma + 1]$ 
3      do  $e \leftarrow \vec{r} \cdot \vec{v}$ 
4          if  $e > 0$ 
5              then return  $True$ 
6          elseif  $e < 0$ 
7              then return  $False$ 
8          else continue
9  return  $True$ 

```

$P$  is the diagonalizing matrix that converts the involutory matrix  $A$  to its standard diagonal form (refer Appendix B). The algorithm assumes that  $P$ , and its inverse  $Pinv$  is available along with the dimensionality of its  $\lambda = -1$  eigensubspace,  $\gamma$ . It computes the last  $\gamma$  coordinates of the vector in descending order ( $\vec{r} \cdot \vec{v}$ ) in the diagonalized basis, which corresponds to that in the  $E_{-1}$  subspace. Since in this subspace, the involutory transformation is essentially an inversion, one needs to check if a negative coordinate is encountered, as per the boolean clause  $\mathcal{B}_\gamma$  (check Appendix B). If it occurs, the vector does not belong to the  $PID$  and  $False$  is returned, otherwise  $True$ .

### 2.3.2 The Universal Approximation Theorem for Involutory Invariant Functions

**Theorem** : Single hidden-layer neural networks can approximate any function  $f : \mathbb{R}^n \rightarrow \mathbb{R}$  that respects an involutory invariance  $f(AX) = pf(X)$  for some  $I_n \neq A \in \mathbb{R}^{n \times n}$  and parity  $p = \pm 1$

**Proof** : It is best encapsulated in the following logical series of statements —

1. A function with an involutory invariance is completely specified by its behaviour in its  $PID$ .
2. All training examples are from the  $PID$  due to reparameterization, which is a normal domain in the mathematical sense.
3. The neural network can approximate, to arbitrary precision, any function in the  $PID$  since it's a universal approximator.
4. The reparameterization encodes the involutory invariance, therefore the neural network can approximate, to arbitrary precision, any involutory invariant function in  $\mathbb{R}^n$ .

### 2.3.3 Handling Affine Transformations

It is possible to learn functions invariant to involutory *affine* transformations as well. A transformation  $T$  is said to be affine if it is of the form  $T = AX + \mu$  for an input  $X \in \mathbb{R}^n$ , and  $A \in \mathbb{R}^{n \times n}$ ,  $\mu \in \mathbb{R}^n$ .

$$\begin{aligned} T^2 X &= IX \\ A(AX + \mu) + \mu &= X \\ A^2 X + (A + I)\mu &= X \end{aligned}$$

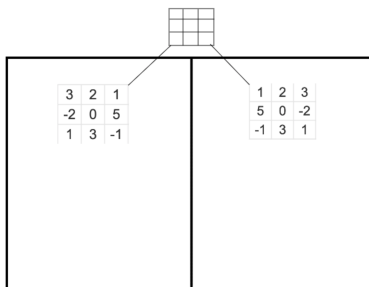


Figure 1: Vertically Symmetric Kernel

An affine transformation  $T$  is involutory *iff*.  $A^2 = I$  and  $A\mu = -\mu$ . Instead of transforming inputs  $X$  by  $T$  directly, it is convenient to shift it as  $X \rightarrow (X - \frac{\mu}{2})$ . It follows that —

$$\begin{aligned} TX &= AX + \mu \\ &= A\left(X - \frac{\mu}{2}\right) + \frac{\mu}{2} \end{aligned}$$

Since  $TX$  would also need to be shifted by  $\frac{\mu}{2}$ , we get —

$$TX \rightarrow \left(TX - \frac{\mu}{2}\right) = A\left(X - \frac{\mu}{2}\right)$$

Thus, the action of an involutory *affine* transformation has been converted to that of an involutory *linear* transformation by a shift of the origin by  $\frac{\mu}{2}$ . The theorems proved, set membership algorithm and the IPT-Net can be used with the same effect after the shift.

## 2.4 Reflection Invariant Kernels for CNN Tasks

For CNN tasks, if it is known beforehand that the images obey an X-reflection or Y-reflection symmetry, it is possible to create reflection invariant feature maps by superimposing the result of two convolutional filters. There are immediate use-cases for such an invariance *i.e.*, human faces are vertically symmetric.

In figure (1), when the filter is convolved about a pixel location  $(x, y)$  of the image, the corresponding vertically-flipped filter is also convolved about the location obtained by reflecting  $(x, y)$  over the vertical mid-plane of the image. The summation of the two convolutions is taken as the pixel value in the output feature map, which ensures that it is invariant to Y-reflections of the input image. In practice, this is done by —

$$\sigma(\text{filter} * \text{image}) + \sigma(\text{filter} * \text{image.flip(axis=1)})$$

where  $\sigma$  is a non-linearity and  $*$  is the non-linear operation. To ensure invariance in X-reflections of the input image, the filter is horizontally flipped instead of vertically. Similarly, when convolving over pixels centred at  $(x, y)$ , it is required to convolve over the location obtained by reflecting  $(x, y)$  about the horizontal mid-plane of the image.

## 3 Experiments

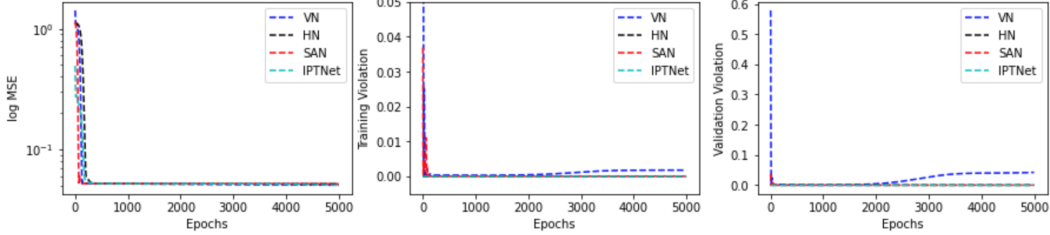
### 3.1 Toy Functions

The four models compared are the following —

1. Vanilla Network (VN)
2. Hub-Layered Network (HN)
3. Symmetrized Activation Network (SAN)
4. IPT Network (IPTNet) — The main contribution of this work

Table 1: Function :  $\sin x$ 

	Loss	Train-Violation	Val-Violation
VN	$4.89 \times 10^{-2} \pm 9.53 \times 10^{-4}$	$2.33 \times 10^{-2} \pm 2.65 \times 10^{-2}$	$1.37 \times 10^{-1} \pm 1.24 \times 10^{-1}$
HN	$6.02 \times 10^{-2} \pm 2.08 \times 10^{-5}$	$0 \pm 0$	$0 \pm 0$
SAN	$6.02 \times 10^{-2} \pm 5.88 \times 10^{-5}$	$1.30 \times 10^{-4} \pm 9.35 \times 10^{-4}$	$1.30 \times 10^{-4} \pm 9.35 \times 10^{-4}$
IPTNet	$5.98 \times 10^{-2} \pm 2.58 \times 10^{-4}$	$0 \pm 0$	$0 \pm 0$

Figure 2: Loss Curve, Training & Validation Violation for  $\sin x$ 

We first test the above models on the 1-D function  $f(x) = \sin x$ . The training set was 100 uniformly chosen points in the interval  $[-1.5, 1.5]$  with each point being displaced by a Gaussian noise of mean 0 and standard deviation 0.25. The validation set chosen was 30 uniformly sampled points in the interval  $[-3, 3]$ . A *violation metric* is computed on either of these sets — it measures the deviation of the function learnt by the network from even/odd symmetry. If this metric is 0, then it indicates that the model perfectly obeys the symmetry. As mentioned in [1], the violation metric for 1-D inversion invariant (*even/odd*) functions is ( $p = \pm 1$ ) —

$$V_p = \frac{1}{M} \sum_{i=1}^M (NN(x_i) - pNN(-x_i))^2$$

where  $x_i$  is an input point belonging to the training or validation set.

The four models above used 2 hidden layers with 10 neurons each and sigmoid activations in between. The number of epochs in the training process was set to 5000 and the learning rate at  $5 \times 10^{-3}$ . In each training instance of the model, we record the following values — the mean squared loss, violation metric on the training set, and violation metric on the validation set. In table (1), we report the mean and standard deviation of these 3 values upon 25 repeated instances of training on the  $\sin x$  function. The final loss in all the models are comparable, however HN and IPTNet report identically 0 violation metric, showing that model respects the invariance exactly. SAN has lower violation than VN, although not identically 0. Figure 2 shows the loss curve, and training/validation violation over the epochs of training. Except VN, the violation metric curve of the other models flatten at 0 from the initial epochs of training. For corresponding results on other 1-D functions, please refer to C. <sup>4</sup>

Next, we test on the 2-D function  $f(x, y) = x \sin y + 1$ . This function is invariant to inversion with parity  $p = 1$  because  $f(x, y) = f(-x, -y)$ . The violation metric (*on the training or validation set*) for a function respecting involution  $A$  is ( $p = \pm 1$ ) —

$$V_{A;p} = \frac{1}{M} \sum_{i=1}^M (NN(X_i) - pNN(AX_i))^2$$

where  $X_i \in \mathbb{R}^n$  is an input point. Figure (3) contains the color-plots of the actual function and the learnt models. With some manual scrutiny, it can be seen that function learnt by Vanilla Net does not respect inversion invariance everywhere. Complete details on the training setup and results on other 2D functions can be found in Appendix C.

<sup>4</sup>All training was done on Google Colab using the GPU runtime environment.



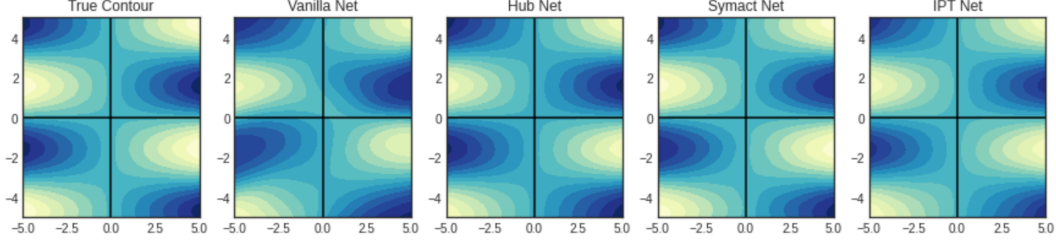


Figure 3:  $f(x, y) = x \sin y + 1$

### 3.2 Image Tasks

We evaluate on the Fashion-MNIST [17] dataset, considering only those 7 classes that have inherent vertical symmetry — *T-shirt/top*, *trouser*, *pullover*, *dress*, *coat*, *shirt*, *bag*. The baseline CNN architecture used was [18]. To convert it into a vertically invariant CNN, the first convolution layer used the vertical reflection-invariant kernel. The training accuracy for the baseline was 86.35%, and that of the symmetric architecture was 86.61%. In terms of testing accuracy, we report 84.55% and 84.95% respectively for baseline/symmetric architecture. More information is present in Appendix C.

## 4 Limitations & Negative Societal Impact

The work is not heavy architecture-wise, but the techniques developed is limited to a highly specific class of invariances. There are other works such as [7, ?] that explore a continuous range of symmetries. Moreover, the scope of application is on those tasks only where a clear symmetry is present on physical grounds. We have tested our techniques on abstract mathematical functions, and were unable to find an appropriate real-life regression dataset to test this upon.

We do not find any direct/indirect negative societal impact of this work because the mathematical notions developed are theoretical and abstract. The toy functions that are primarily tested are purely mathematical, and the CNN task used is well known without an obvious negative impact.

## 5 Future Works

It would be interesting to parameterize the class of safe activation functions with learnable parameters. This allows the network to suitably learn an activation function given the underlying involutory matrix  $A$ . There needs to be further exploration of the connection between activation functions and expressivity of neural networks as has been done in section (2.2.1). The discrete rotation matrix  $R_k$  is also a physically relevant transformation in 2 dimensions.  $k$  is the number of sectors into which the plane is divided ( $\theta = \frac{2\pi}{k}$ ) —

$$R_k = \begin{bmatrix} \cos \theta & -\sin \theta \\ \sin \theta & \cos \theta \end{bmatrix}$$

In order to make a neural network invariant to the action of a discrete rotation  $R_k$ , two approaches are possible.

**Rotation Invariant Hub Layer** - The hub layer computes a superposition of activation values of the form ( $X \in \mathbb{R}^2$ ) —

$$H(X) = h(X) + h(R_k X) + h(R_k^2 X) + \dots + h(R_k^{k-1} X)$$

**Rotation Invariant Activations** - The first hidden layer uses a superposition of activation functions of the form —

$$\sigma(w^T X + b) + \sigma(w^T R_k X + b) + \sigma(w^T R_k^2 X + b) + \dots + \sigma(w^T R_k^{k-1} X + b)$$

The matrix  $R_k$  is  $k$ -involutory because  $R_k^k = I$ . It is crucial to assess the behaviour of the sum of activation functions as given above, in a manner similar to section 2.2.1. The analysis in this

work would be a special case of generic  $k$ -involutory matrices with  $k = 2$ . Moreover, an analogous construction of rotation invariant kernels for CNN tasks can also be done.

Using the techniques of Lagaris [19] and NeuroDiffEq [20], an architecture can be built to solve PDEs that are invariant to sign inversion, or invariant to an involutory transformation. Involutory symmetries can also be imposed on Hamiltonian Neural Network [21]. Hamiltonians of many problems important to Physics are invariant to sign inversion of the canonical coordinates *e.g.*, harmonic oscillator, pendulum *etc.*.

## 6 Conclusion

We have developed the necessary mathematical background, theorems, and architectures for neural networks to learn functions that obey an involutory invariance. Additionally, we analysed symmetric sums of activation functions and their expressiveness. The models were tested on multiple toy functions and the invariance-respecting property was confirmed via experiments. An adaption of these techniques to vertical/horizontal reflection in CNN tasks was also demonstrated.

## References

- [1] M. Mattheakis, P. Protopapas, D. Sondak, M. Di Giovanni, and E. Kaxiras. Physical symmetries embedded in neural networks, 2020.
- [2] Rui Wang, Robin Walters, and Rose Yu. Incorporating symmetry into deep dynamics models for improved generalization, 2021.
- [3] Alexander Bogatskiy, Brandon Anderson, Jan T. Offermann, Marwah Roussi, David W. Miller, and Risi Kondor. Lorentz group equivariant neural network for particle physics, 2020.
- [4] R. Resnick. *Introduction to Special Relativity*. Wiley, 1968.
- [5] Gabriela Barenboim, Johannes Hirn, and Veronica Sanz. Symmetry meets ai, 2021.
- [6] Emma Slade and Francesco Farina. Beyond permutation equivariance in graph networks, 2021.
- [7] Carlos Esteves, Christine Allen-Blanchette, Ameesh Makadia, and Kostas Daniilidis. Learning  $so(3)$  equivariant representations with spherical cnns, 2018.
- [8] Taco S. Cohen and Max Welling. Group equivariant convolutional networks, 2016.
- [9] Risi Kondor and Shubhendu Trivedi. On the generalization of equivariance and convolution in neural networks to the action of compact groups, 2018.
- [10] D. E. Rumelhart, G. E. Hinton, and R. J. Williams. *Learning Internal Representations by Error Propagation*, page 318–362. MIT Press, Cambridge, MA, USA, 1986.
- [11] G. Cybenko. Approximation by superpositions of a sigmoidal function. *Mathematics of Control, Signals, and Systems (MCSS)*, 2(4):303–314, December 1989.
- [12] Patrick Kidger and Terry Lyons. Universal approximation with deep narrow networks, 2020.
- [13] Liu Ziyin, Tilman Hartwig, and Masahito Ueda. Neural networks fail to learn periodic functions and how to fix it, 2020.
- [14] Vinod Nair and Geoffrey E. Hinton. Rectified linear units improve restricted boltzmann machines. In *Proceedings of the 27th International Conference on International Conference on Machine Learning, ICML'10*, page 807–814, Madison, WI, USA, 2010. Omnipress.
- [15] Prajit Ramachandran, Barret Zoph, and Quoc V. Le. Searching for activation functions, 2017.
- [16] Hao Zheng, Zhanlei Yang, Wenju Liu, Jizhong Liang, and Yanpeng Li. Improving deep neural networks using softplus units. In *2015 International Joint Conference on Neural Networks (IJCNN)*, pages 1–4, 2015.
- [17] Han Xiao, Kashif Rasul, and Roland Vollgraf. Fashion-mnist: a novel image dataset for benchmarking machine learning algorithms, 2017.
- [18] Let’s build a fashion-mnist cnn, pytorch style. <https://towardsdatascience.com/build-a-fashion-mnist-cnn-pytorch-style-efb297e22582>. Accessed: 2021-05-28.
- [19] I. E. Lagaris, A. Likas, and D. I. Fotiadis. Artificial neural networks for solving ordinary and partial differential equations. *IEEE Transactions on Neural Networks*, 9(5):987–1000, 1998.

- [20] Feiyu Chen, David Sondak, Pavlos Protopapas, Marios Mattheakis, Shuheng Liu, Devansh Agarwal, and Marco Di Giovanni. Neurodifreq: A python package for solving differential equations with neural networks. *Journal of Open Source Software*, 5(46):1931, 2020.
- [21] Sam Greydanus, Misko Dzamba, and Jason Yosinski. Hamiltonian neural networks, 2019.
- [22] Fuzhen Zhang. *Special Types of Matrices*, pages 125–170. Springer New York, New York, NY, 2011.
- [23] Gilbert Strang. *Introduction to Linear Algebra*. Wellesley-Cambridge Press, Wellesley, MA, fourth edition, 2009.

## A Linear Algebra Recap

We first state some elementary results from Linear Algebra and the theory of matrices. Using these, we state the *Involutory Partition Theorem* that is conducive to proving a Universal Approximation Theorem in class of functions  $C_A = \{f \mid f : \mathbb{R}^n \rightarrow \mathbb{R} \ni f(AX) = f(X) \forall X \in \text{Dom}(f) \subseteq \mathbb{R}^n\}$

$A \in \mathbb{R}^{n \times n}$  and  $f$  is a function that respects an involutory invariance in its respective domain. One of our proposed architectures (Section 2.3) is based on this theorem, and as a consequence, enjoys approximation properties to arbitrary precision.

**Result 1** : *Involutory matrices can only have eigenvalues  $\lambda = \pm 1$ .*

**Proof** : Consider the eigenvalue equation —

$$\begin{aligned} AX &= \lambda X \\ A^2X &= \lambda(AX) \\ IX &= \lambda^2 X \\ (\lambda^2 - 1)X &= 0 \end{aligned}$$

Since the above relation holds for all eigenvectors  $X$ , we obtain —

$$\begin{aligned} \lambda^2 - 1 &= 0 \\ \implies \lambda &= \pm 1 \end{aligned}$$

*Caveat* : Not all involutory matrices have both eigenvalues  $\pm 1$ . For instance,  $-I_n$  has  $\lambda = -1$  as its only eigenvalue, and  $I_n$  only has  $\lambda = 1$ .

**Result 2** : *A matrix is involutory iff. it is similar to a diagonal matrix of the following form  $\text{diag}(1, 1, \dots, 1, -1, -1, \dots, -1)$*

**Proof** : Please refer to Theorem 5.1 in [22] for the proof.

*Caveat* : The only matrices similar to  $\pm I_n$  are themselves. Let  $A$  be related to  $\pm I_n$  by a similarity transformation (for some invertible  $P \in \mathbb{R}^{n \times n}$ ) —

$$\begin{aligned} A &= \pm P^{-1} I_n P \\ &= \pm (P^{-1} I_n) P \\ &= \pm P^{-1} P \\ &= \pm I_n \end{aligned}$$

**Corollary 2** : All involutory matrices except  $\pm I_n$  have both eigenvalues  $\lambda = \pm 1$ . This is immediately obvious from the aforementioned caveat, as its diagonalized form is neither  $\text{diag}(1, \dots, 1)$  nor  $\text{diag}(-1, \dots, -1)$ . Thus the matrices strictly possess non-empty eigensubspaces  $A_1$  and  $A_{-1}$ .

**Result 3** : *Similarity Transformation of a matrix preserve its eigenvalues, and their corresponding algebraic/geometric multiplicities.*

**Proof** : This is obvious from intuition as all similarity transformations represent a change of basis, which is unrelated to the geometric properties of the matrix. It is a standard result in matrix theory and the reader is referred to [23].

**Result 4** : *The combined eigensubspaces of involutory matrices  $\in \mathbb{R}^{n \times n}$  span all of  $\mathbb{R}^n$ .*

**Proof** : If the involutory matrix  $A$  under consideration is  $\pm I_n$ , there exists only one eigensubspace  $A_{\pm 1}$  and it clearly spans  $\mathbb{R}^n$ . On the other hand for  $A \neq \pm I_n$ , let  $E$  be the diagonal matrix to which  $A$  is similar by the relation  $E = P^{-1}AP$  for some invertible matrix  $P \in \mathbb{R}^{n \times n}$ . Let the 1 entries in the main diagonal of  $E$  be upto some row  $k < n$ , beyond which all entries are  $-1$ . Then —

$$\begin{aligned} E_1 &= \text{span}\{\vec{e}_i \mid 1 \leq i \leq k\} \\ E_{-1} &= \text{span}\{\vec{e}_i \mid k < i \leq n\} \end{aligned}$$

Moreover,

$$\begin{aligned} \dim(E_1) &= k \\ \dim(E_{-1}) &= n - k \end{aligned}$$

It is easily seen that  $\text{span}(E_1 \cup E_{-1}) = \text{span}\{\vec{e}_i \mid 1 \leq i \leq n\} = \mathbb{R}^n$ . Due to the similarity transformation, we obtain —

$$\begin{aligned} A_1 &= \text{span}\{P^{-1}\vec{e}_i \mid \vec{e}_i \in E_1\} \\ A_{-1} &= \text{span}\{P^{-1}\vec{e}_i \mid \vec{e}_i \in E_{-1}\} \end{aligned}$$

Because geometric multiplicities are preserved —

$$\begin{aligned} \dim(A_1) &= \dim(E_1) = k \\ \dim(A_{-1}) &= \dim(E_{-1}) = n - k \end{aligned}$$

Finally, combining the fact that eigenvectors belonging to different eigenspaces are linearly independent, we obtain the final result —

$$\text{span}(A_1 \cup A_{-1}) = \mathbb{R}^n$$

## B Involutory Partition Theorem

**Theorem** : An involutory matrix  $A \neq I_n$  partitions  $\mathbb{R}^n$  into three mutually exclusive non-empty subsets  $S_0, S_+, S_-$ , with the following properties —

1.  $\forall \vec{v} \in S_0, A\vec{v} = \vec{v}$
2.  $\forall \vec{v} \in S_+, A\vec{v} \in S_-$
3.  $\forall \vec{v} \in S_-, A\vec{v} \in S_+$

**Proof** : The proof is by construction and we consider the two cases  $A \neq -I_n$  and  $A = -I_n$  respectively<sup>5</sup>. In each case, must show the following hold —

1. Partition Property -  $S_0 \cup S_+ \cup S_- = \mathbb{R}^n$
2. Mutual Exclusion Property -  $S_0 \cap S_+ = S_+ \cap S_- = S_0 \cap S_- = \Phi$
3. Imaging Properties - Statements 1, 2 and 3 of the theorem.

• *Case One* ( $A = -I_n$ ) — This case is proved via induction on the dimension  $n$ .

**Induction Hypothesis** : Let the hypothesis  $P(n)$  be the following set of statements —

$$\begin{aligned} S_0^{(n)} &= \{\vec{0}_n\} \\ S_+^{(n)} &= \left\{ \sum_{i=1}^n \alpha_i \vec{e}_i \mid \alpha_1, \dots, \alpha_n \in \mathbb{R}; \mathcal{A}_n \right\} \\ S_-^{(n)} &= \left\{ \sum_{i=1}^n \beta_i \vec{e}_i \mid \beta_1, \dots, \beta_n \in \mathbb{R}; \mathcal{B}_n \right\} \end{aligned}$$

---

<sup>5</sup>The point of contention, more precisely, is whether  $A$  is similar to  $-I_n$ .

where  $\vec{0}_n$  is the zero vector in  $\mathbb{R}^n$ .  $\vec{e}_i$  is the natural basis vectors<sup>6</sup> in  $n$  dimensions and  $\mathcal{A}_n, \mathcal{B}_n$  are boolean clauses on the co-efficients  $\alpha_i, \beta_i$  respectively —

$$\mathcal{A}_n = \begin{cases} \alpha_1 > 0 & n = 1 \\ (\alpha_n > 0) \vee (\alpha_n = 0 \wedge \mathcal{A}_{n-1}) & n \geq 2 \end{cases}$$

$$\mathcal{B}_n = \begin{cases} \beta_1 < 0 & n = 1 \\ (\beta_n < 0) \vee (\beta_n = 0 \wedge \mathcal{B}_{n-1}) & n \geq 2 \end{cases}$$

**Base Case** ( $n = 1$ ): The subsets are —

$$S_0^{(1)} = \{0\}$$

$$S_+^{(1)} = \{\alpha_1 \vec{e}_1 \mid \alpha_1 > 0\} \equiv \{x > 0 \mid x \in \mathbb{R}\}$$

$$S_-^{(1)} = \{\beta_1 \vec{e}_1 \mid \beta_1 < 0\} \equiv \{x < 0 \mid x \in \mathbb{R}\}$$

This is the real number line divided into the negative reals, the singleton subset containing zero, and the positive reals. It is trivial to see that the partition, mutual exclusion and defining properties hold.

**Inductive Step** : We show that  $P(k)$  is true, assuming  $P(k-1)$  is true for some  $k \in \mathbb{N}$ . Define  $v_i$  to be the  $i^{\text{th}}$  component of the vector  $\vec{v}$ . Let us restrict ourselves to the subspace  $v_k = 0$  —

$$T_0^{(k)} = \{\vec{v} \mid \vec{v} \in \mathbb{R}^n, v_k = 0\}$$

This corresponds to the case of  $\alpha_k = \beta_k = 0$  and one can state the following logical equivalences —

$$\alpha_k = 0 \vdash \mathcal{A}_k \equiv (\alpha_k > 0) \vee (\alpha_k = 0 \wedge \mathcal{A}_{k-1}) \equiv \mathcal{A}_{k-1}$$

$$\beta_k = 0 \vdash \mathcal{B}_k \equiv (\beta_k < 0) \vee (\beta_k = 0 \wedge \mathcal{B}_{k-1}) \equiv \mathcal{B}_{k-1}$$

Finally, upon expanding  $\mathcal{A}_{k-1}, \mathcal{B}_{k-1}$  by their recursive definitions —

$$T_+^{(k)} \equiv S_+^{(k)} \Big|_{v_k=0} = \left\{ \sum_{i=1}^{k-1} \alpha_i \vec{e}_i \mid \alpha_1, \dots, \alpha_{k-1} \in \mathbb{R}; \mathcal{A}_{k-1} \right\} \approx S_+^{(k-1)}$$

$$T_-^{(k)} \equiv S_-^{(k)} \Big|_{v_k=0} = \left\{ \sum_{i=1}^{k-1} \beta_i \vec{e}_i \mid \beta_1, \dots, \beta_{k-1} \in \mathbb{R}; \mathcal{B}_{k-1} \right\} \approx S_-^{(k-1)}$$

By our induction hypothesis  $T_+^{(k)}, T_-^{(k)}$  automatically satisfy the mutual exclusion, partition and statements 2, 3 of the theorem.<sup>7</sup> Moreover,  $\vec{0}_k \notin T_+^{(k)}, T_-^{(k)}$  as it would require  $\alpha_k, \alpha_{k-1}, \dots, \alpha_2 = 0$  or  $\beta_k, \beta_{k-1}, \dots, \beta_2 = 0$  which would recurse down to the basic boolean clauses  $\mathcal{A}_1 \equiv \alpha_1 > 0$  and  $\mathcal{B}_1 \equiv \beta_1 < 0$  respectively, disallowing the zero vector  $\vec{0}_k$ .

We are now left with vectors  $\vec{v}$  having  $v_k \neq 0$  —

$$U_0^{(k)} = \{\vec{v} \mid \vec{v} \in \mathbb{R}^k, v_k \neq 0\}$$

This corresponds to the case of  $\alpha_k \neq 0$  and  $\beta_k \neq 0$  and similar logical equivalences can be stated —

$$\alpha_k \neq 0 \vdash \mathcal{A}_k \equiv (\alpha_k > 0) \vee (\alpha_k = 0 \wedge \mathcal{A}_{k-1}) \equiv \alpha_k > 0$$

$$\beta_k \neq 0 \vdash \mathcal{B}_k \equiv (\beta_k < 0) \vee (\beta_k = 0 \wedge \mathcal{B}_{k-1}) \equiv \beta_k < 0$$

<sup>6</sup>The proof holds in any basis that spans  $\mathbb{R}^n$ . Similarity matrices  $P \in \mathbb{R}^{n \times n}$  represent a change of basis, and  $-I_n$  is unaffected similarity transformations. Hence, the action of inversion (*coordinate sign flip*) in the natural basis is retained in any other basis.

<sup>7</sup>The reason for using the  $\approx$  symbol is that bonafide  $S_+^{(k-1)}, S_-^{(k-1)}$  would use natural basis vectors  $\vec{e}_i \in \mathbb{R}^{k-1}$ , whereas we instead have  $\vec{e}_i \in \mathbb{R}^k$  for  $i \in \{1, 2, \dots, k-1\}$ . This is equivalent to using the basis vectors of  $\mathbb{R}^{k-1}$  with a 0 appended as an "extra" dimension at the end of each vector. The usage of the  $\approx$  sign is not rigorous, but it has only been used to exemplify how the proof by induction work.  $S_{\pm}^{(k)}$  truly depends on  $S_{\pm}^{(k-1)}$  with an extra dimension of 0 padded to every vector belonging to the latter.

Our subsets of interest take the form —

$$U_+^{(k)} \equiv S_+^{(k)} \Big|_{v_k \neq 0} = \left\{ \sum_{i=1}^{k-1} \alpha_i \vec{e}_i + \alpha_k \vec{e}_k \mid \alpha_1, \dots, \alpha_{k-1} \in \mathbb{R}; \alpha_k > 0 \right\}$$

$$U_-^{(k)} \equiv S_-^{(k)} \Big|_{v_k \neq 0} = \left\{ \sum_{i=1}^{k-1} \beta_i \vec{e}_i + \beta_k \vec{e}_k \mid \beta_1, \dots, \beta_{k-1} \in \mathbb{R}; \beta_k < 0 \right\}$$

**Mutual Exclusion Property** - It is impossible for the above sets to have any common vector because one requires  $v_k > 0$  and the other  $v_k < 0$ . This also implies that  $\vec{\mathbf{0}}_k$  does not belong to either set. Hence  $U_+^{(k)} \cap U_-^{(k)} = \Phi$ .

**Partition Property** - One set contains all vectors in the positive  $\vec{e}_k$ -hyperoctants and the other contains those in the negative  $\vec{e}_k$ -hyperoctants. Thus, we have  $U_+^{(k)} \cup U_-^{(k)} = U_0^{(k)}$

**Imaging Properties** - For any vector  $\vec{v} = [\alpha_1, \alpha_2, \dots, \alpha_k]^T \in U_+^{(k)}$ , we have —

$$A\vec{v} = [-\alpha_1, -\alpha_2, \dots, -\alpha_k]^T \in U_-^{(k)}$$

as one can set  $\beta_i = -\alpha_i$  and  $\alpha_k > 0 \implies \beta_k < 0$  clearly satisfying the definition of  $U_-^{(k)}$ .

Analogously, one can choose a vector  $\vec{v} \in U_-^{(k)}$  and show that  $A\vec{v} \in U_+^{(k)}$ . Hence statements 2, 3 are also satisfied.

Finally, we note that —

$$S_+^{(k)} = S_+^{(k)} \Big|_{v_k=0} \cup S_+^{(k)} \Big|_{v_k \neq 0} = T_+^{(k)} \cup U_+^{(k)}$$

$$S_-^{(k)} = S_-^{(k)} \Big|_{v_k=0} \cup S_-^{(k)} \Big|_{v_k \neq 0} = T_-^{(k)} \cup U_-^{(k)}$$

Since the mutual exclusion, partition and statement 2, 3 of the theorem hold for  $T_{\pm}^{(k)}$  and  $U_{\pm}^{(k)}$  among themselves, it must also hold for  $S_+^{(k)}$  and  $S_-^{(k)}$ . The set  $S_0^{(k)} = \{\vec{\mathbf{0}}_k\}$  is a singleton set and trivially satisfies statement 1. Hence  $P(k-1) \implies P(k)$  and this completes part of the proof.

• *Case Two* ( $A \neq -I_n$ ) — By a suitable similarity transformation  $P \in \mathbb{R}^{n \times n}$ , the matrix  $A$  can be diagonalized to the form —

$$\underbrace{\text{diag}(1, \dots, 1, -1, \dots, -1)}_{k \text{ times}}$$

Let  $E = P^{-1}AP$ , and we consider the eigensubspaces  $E_{\pm 1}$  that have dimensionality  $k$  and  $(n-k)$  respectively. Let the natural basis after the similarity transformation be  $\{\vec{e}'_i\}$ . We have —

$$E_1 = \text{span}\{\vec{e}'_i \mid 1 \leq i \leq k\}$$

$$E_{-1} = \text{span}\{\vec{e}'_i \mid k < i \leq n\}$$

The important observation here is that vectors in  $E_{-1}$  transform<sup>8</sup> as  $-I_{n-k}$  under  $A$ . Hence, the subspace  $E_{-1}$  obeys the involutory partition theorem (*Case One*) and can be split into three parts —  $E_{-1}^{(-)}, E_{-1}^{(0)}, E_{-1}^{(+)}$ . We first define the sets  $S'$  as<sup>9</sup> —

$$S'_- = E_1 \otimes E_{-1}^{(-)}$$

$$S'_0 = E_1 \otimes E_{-1}^{(0)}$$

$$S'_+ = E_1 \otimes E_{-1}^{(+)}$$

<sup>8</sup>An arbitrary vector will have the first  $k$  entries in its coordinates as 0.

<sup>9</sup>Cartesian Product, in this context, is defined as  $Z_1 \otimes Z_2 = \{\vec{v}_1 + \vec{v}_2 \mid \vec{v}_1 \in Z_1, \vec{v}_2 \in Z_2\}$ . This is legitimate, because in each appearance of such a product, the two sets are eigenspaces whose vectors reside in independent dimensions.

We claim that the sets  $S$  obey the involutory partition theorem —

$$\begin{aligned} S_- &= \{P\vec{v}' \mid \vec{v}' \in S'_-\} \\ S_0 &= \{P\vec{v}' \mid \vec{v}' \in S'_0\} \\ S_+ &= \{P\vec{v}' \mid \vec{v}' \in S'_+\} \end{aligned}$$

**Mutual Exclusion Property** - Since the subspace  $E_{-1}$  satisfies the mutual exclusion property,  $S'_-, S'_0, S'_+$  also do. The transformation of the  $S'$  sets, by the similarity matrix  $P$ , to the  $S$  sets cannot break mutual exclusion as it only represents a change of basis.

**Partition Property** - The  $S'$  sets obey the property because —

$$\begin{aligned} \mathbb{R}^n &= E_1 \otimes E_{-1} \\ &= E_1 \otimes \left( E_{-1}^{(-)} \cup E_{-1}^{(0)} \cup E_{-1}^{(+)} \right) && \text{(Partition Theorem)} \\ &= \left( E_1 \otimes E_{-1}^{(-)} \right) \cup \left( E_1 \otimes E_{-1}^{(0)} \right) \cup \left( E_1 \otimes E_{-1}^{(+)} \right) && (\otimes \text{ distribues over } \cup) \\ &= S'_- \cup S'_0 \cup S'_+ \end{aligned}$$

By a similar argument, transformation from  $S' \rightarrow S$  by  $P$  cannot break the property.

**Imaging Properties** - Before proceeding, we note that  $E = P^{-1}AP \implies PE = AP$ . Consider a vector  $\vec{v} \in S'_0$ , it is of the form  $\vec{v} = P(\vec{v}'_1 + \vec{v}'_{-1})$  for  $\vec{v}'_1 \in E_1$  and  $\vec{v}'_{-1} \in E_{-1}^{(0)}$  that satisfies  $E\vec{v}'_{-1} = \vec{v}'_{-1}$  —

$$\begin{aligned} A\vec{v} &= AP(\vec{v}'_1 + \vec{v}'_{-1}) \\ &= PE(\vec{v}'_1 + \vec{v}'_{-1}) \\ &= P(\vec{v}'_1 + \vec{v}'_{-1}) \\ &= \vec{v} \end{aligned}$$

Hence, statement 1 of the theorem holds. To see the validity of statement 2, consider a  $\vec{v} \in S'_+$  of the same form except  $\vec{v}'_{-1} \in E_{-1}^{(+)}$  —

$$\begin{aligned} A\vec{v} &= AP(\vec{v}'_1 + \vec{v}'_{-1}) \\ &= PE(\vec{v}'_1 + \vec{v}'_{-1}) \\ &= P(\vec{v}'_1 + \vec{w}'_{-1}) \end{aligned}$$

where  $\vec{w}'_{-1} \in E_{-1}^{(-)}$  because  $E_{-1}$  satisfies statement 2 of the theorem. Thus  $\vec{v}'_1 + \vec{w}'_{-1} \in S'_-$  and it is clear that  $A\vec{v} \in S_-$ . A similar argument can be drawn starting from a vector  $\vec{v}' \in S'_-$  instead, and statement 3 can be proved.

## C Complete Results

Source code to the results can be found in this anonymous google drive folder. <sup>10 11</sup>

### C.1 1D Functions

We provide training results on two other 1-D functions  $f(x) = \cos x$  and  $f(x) = x \cos x$  in table (2) and table (3) respectively. The loss/violation curves can be found in figures (4) and (5) respectively. The Vanilla Net achieves a lower loss, but a better fit to the training points does not necessarily imply higher obedience (*smaller violation*) to the symmetry. The results obtained can be verified by running the `1D-Results.ipynb` notebook in the anonymous folder.

<sup>10</sup><https://drive.google.com/drive/folders/15-7Y3B8t6ScvEca8FqXxTmG-iQi-eNv8> is a link to an anonymous google folder containing the code/results

<sup>11</sup>Ensure to use the GPU runtime on Google Colab.

Table 2: Function :  $\cos x$ 

	Loss	Train-Violation	Val-Violation
VN	$6.58 \times 10^{-2} \pm 3.13 \times 10^{-4}$	$2.79 \times 10^{-3} \pm 2.07 \times 10^{-3}$	$8.37 \times 10^{-3} \pm 9.98 \times 10^{-3}$
HN	$8.98 \times 10^{-2} \pm 5.68 \times 10^{-2}$	$0 \pm 0$	$0 \pm 0$
SAN	$6.74 \times 10^{-2} \pm 1.14 \times 10^{-3}$	$0 \pm 0$	$0 \pm 0$
IPTNet	$6.78 \times 10^{-2} \pm 2.26 \times 10^{-4}$	$0 \pm 0$	$0 \pm 0$

Table 3: Function :  $x \cos x$ 

	Loss	Train-Violation	Val-Violation
VN	$6.36 \times 10^{-2} \pm 1.29 \times 10^{-3}$	$3.45 \times 10^{-3} \pm 1.51 \times 10^{-3}$	$5.55 \times 10^{-2} \pm 4.11 \times 10^{-2}$
HN	$8.16 \times 10^{-2} \pm 1.04 \times 10^{-2}$	$0 \pm 0$	$0 \pm 0$
SAN	$6.48 \times 10^{-2} \pm 2.03 \times 10^{-3}$	$4.63 \times 10^{-4} \pm 3.24 \times 10^{-4}$	$4.63 \times 10^{-4} \pm 3.24 \times 10^{-4}$
IPTNet	$6.56 \times 10^{-2} \pm 1.56 \times 10^{-3}$	$0 \pm 0$	$0 \pm 0$

## C.2 2D Functions

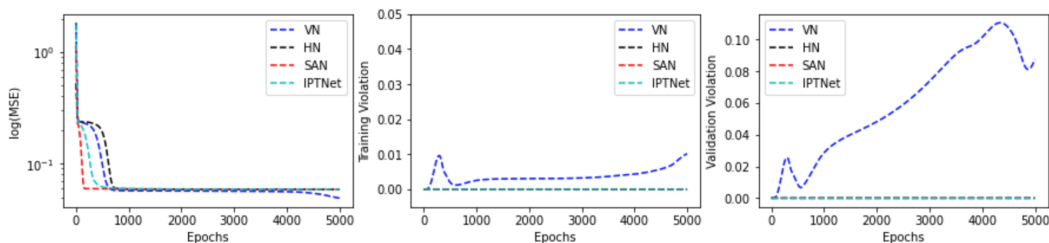
The training set is 1000 randomly chosen points within the grid  $[-5, 5] \times [-5, 5]$ . See figure (6) for the visualized training set. Table (4) enlists the functions that have been used for testing. Evenly spaced grid points in  $[-5, 5] \times [-5, 5]$  was used as the validation set. The contours of function 12 are in table (4) in figure (7) and the loss/violation curves in figure (8). For function 14, please refer to figure (9) and (10). The quoted results can be verified, and results on the other function obtained, by running the `2D-Contours-and-Results.ipynb` notebook in the anonymous folder.

## C.3 FashionMNIST

The baseline CNN used features two convolutional layers (*with maxpool*), followed by two fully connected layers and a softmax unit with cross-entropy loss. To convert this architecture into a vertically symmetric one, the kernels of the first convolutional layer are symmetrized according to section (3.2). Table (5) enlists the various hyperparameters settings under which the training was conducting, and the final loss, train/test accuracies.

The subset of classes chosen for our tasks exhibit vertical symmetry. Thus, if any arbitrary image is vertically flipped before passing onto the network, it is expected that identical feature maps would be computed. This is true for the Symmetric CNN model as vertically symmetric kernel is used in the first convolutional layer, which encodes the inherent physical symmetry of the task. On the other hand, for the baseline CNN model, it is not expected that identical feature maps are computed upon flipping the image. In figure (11) and (12), The baseline CNN does not compute identical maps upon flipping the input, whereas the symmetric model does.

The results of this section can be verified by running the notebook named `Fashion-MNIST.ipynb` in the anonymous folder.

Figure 4: Loss Curve, Training & Validation Violation for  $\cos x$



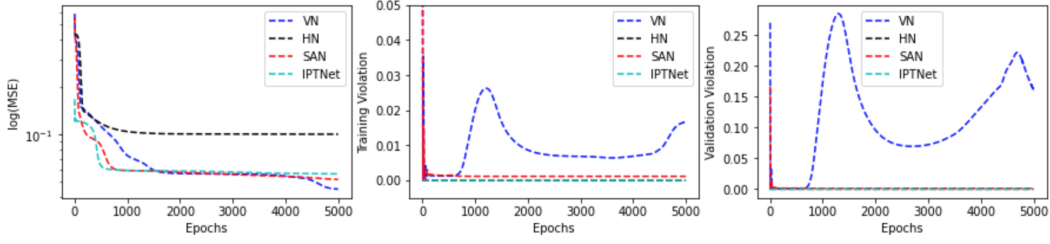


Figure 5: Loss Curve, Training & Validation Violation for  $x \cos x$

Table 4: List of 2-D functions and their involutions

Involution	No.	Function	Parity
$\begin{bmatrix} 1 & 0 \\ 0 & -1 \end{bmatrix}$	1.	$y^2 - x$	+1
	2.	$x \cos y$	+1
	3.	$x \sin y$	-1
$\begin{bmatrix} -1 & 0 \\ 0 & 1 \end{bmatrix}$	4.	$x^2 - y$	+1
	5.	$y \cos x$	+1
	6.	$y \sin x$	-1
$\begin{bmatrix} -1 & 0 \\ 0 & -1 \end{bmatrix}$	7.	$x \sin y + 1$	+1
	8.	$y \sin x + 1$	+1
	9.	$(x + y)/10$	-1
$\begin{bmatrix} 0 & 1 \\ 1 & 0 \end{bmatrix}$	10.	$(x + y)/10$	+1
	11.	$\sin x + \sin y$	+1
	12.	$\sin x - \sin y$	-1
$\begin{bmatrix} \frac{1}{2} & 3 \\ \frac{1}{4} & -\frac{1}{2} \end{bmatrix}$	13.	$(x + 2y)/15$	+1
	14.	$x \sin y + (x/2 + 3y) \sin(x/4 - y/2)$	+1
	15.	$x \sin y - (x/2 + 3y) \sin(x/4 - y/2)$	-1

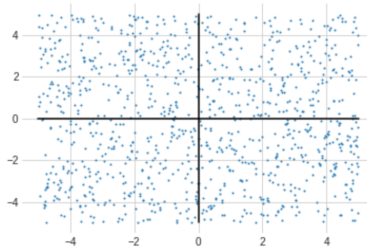


Figure 6: 2D Training Set

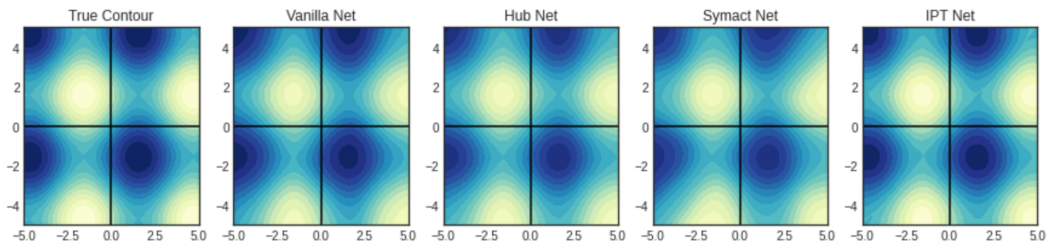


Figure 7: Function 12 Contours

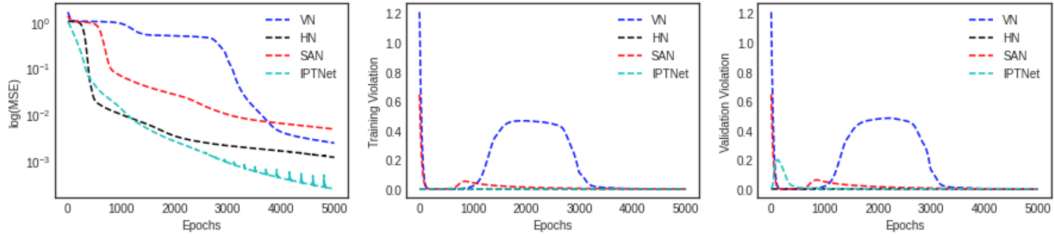


Figure 8: Function 12 Loss/Violation Curves

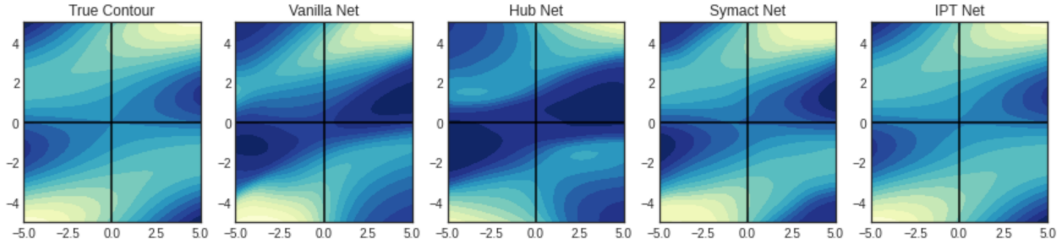


Figure 9: Function 14 Contours

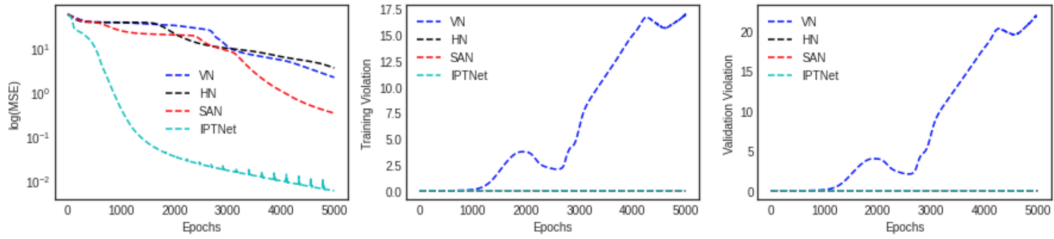


Figure 10: Function 14 Loss/Violation Curves

Table 5: Baseline vs. Symmetric CNN

Learning Rate	Batch Size	Shuffle	Baseline CNN			Symmetric CNN		
			Loss	Train Acc.	Test Acc.	Loss	Train Acc.	Test Acc.
0.01	100	True	0.351	86.75%	84.8%	0.354	86.63%	84.92%
0.01	100	False	0.370	86.09%	84.24%	0.356	86.72%	84.7%
0.01	1000	True	0.387	85.70%	84.62%	0.374	86.23%	85.77%
0.01	1000	False	0.383	85.78%	85.01%	0.343	86.96%	85.31%
0.001	100	True	0.377	86.08%	84.62%	0.356	86.82%	85.64%
0.001	100	False	0.384	85.72%	84.88%	0.354	87.05%	85.67%
0.001	1000	True	0.640	75.69%	74.90%	0.591	77.77%	77.5%
0.001	1000	False	0.595	78.78%	77.98%	0.505	81.76%	81.17%

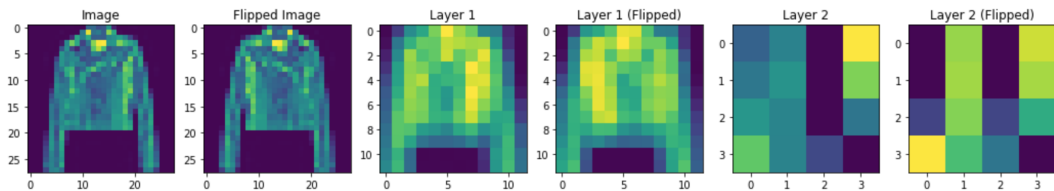


Figure 11: Baseline CNN Feature Maps

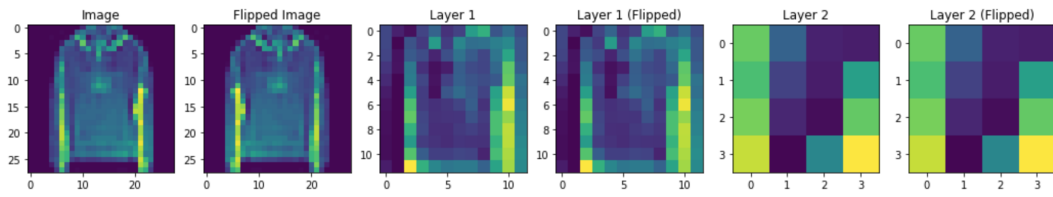


Figure 12: Symmetric CNN Feature Maps